N72-23055

NASA TECHNICAL MEMORANDUM

NASA TM X-68057

NASA TM X-68057

SILICON SOLAR CELL EFFICIENCY - PRACTICE AND PROMISE

by Henry W. Brandhorst, Jr.
Lewis Research Center
Cleveland, Ohio

TECHNICAL PAPER proposed for presentation at
Ninth Photovoltaic Specialists Conference
Silver Spring, Maryland, May 2-5, 1972

SILICON SOLAR CELL EFFICIENCY - PRACTICE AND PROMISE

by Henry W. Brandhorst, Jr.

Lewis Research Center
National Aeronautics and Space Administration
Cleveland, Ohio

E-6915

ABSTRACT

The maximum efficiency of silicon solar cells is calculated and yields a value near 18%. Additionally, the performance of these high efficiency cells in a synchronous orbit radiation field is calculated and indicates that these cells would be superior to present silicon cells at all times. The performance of conventional cells is analyzed and several areas in which performance gains may be achieved are discussed. These areas include improvements in diffused region profile, in reduction of excess forward currents in cells made from low resistivity material and in the theory for describing complex solar cell structures.

INTRODUCTION

Over the last several years, interest in the maximum efficiency of silicon solar cells has been reawakened. Previous studies (1, 2) concluded a maximum efficiency of 22% and indicated several areas in need of study before this efficiency could be achieved. It is the purpose of this paper to repeat these efficiency calculations with more realistic loss terms due to reflection and grid coverage and a more general expression for the reverse saturation current. Next, because cells are widely used in a space environment, the performance of these improved cells in a synchronous orbit radiation field was calculated. Finally, the performance of present cells was analyzed in terms of present theories to determine areas which hold the most promise of yielding significant gains in efficiency.

THEORY AND CALCULATIONS

The purpose of this section is to determine the maximum practical efficiency of a silicon cell. The power output, P_{max} of the cell (and hence its efficiency) can be written in the following way:

$$P_{max} = F.F. \times I_{sc} \times V_{oc}$$

where F.F. is fill factor, I_{sc} is the short-circuit current and V_{oc} is the open-circuit voltage. Raising any of the three quantities increases the power output. In general, the open-circuit voltage can be increased by reducing the resistivity. The short-circuit current can be increased by increasing the base minority carrier lifetime, by decreasing recombination at the surface of the cell, and by decreasing both surface reflection and front contact shadowing. The fill factor can be raised by reducing the series resistance and improving the junction characteristics. In the ensuing pages attention will be directed toward all these avenues to raising efficiency.

Efficiency Calculations

Diode Equation: The starting point for the ultimate efficiency calculations was the simple diode equation:

$$I = I_o(e^{\frac{qV}{kT}}-1)-I_L \tag{1}$$

where I is the current, I_o is the reverse saturation current calculated from diffusion theory, V is voltage, q is electronic charge, k is Boltzmann's constant, T is the absolute temperature (°K) and I_L is the light generated current. Because diffusion theory is being used, the A value generally shown in equation (1) equals unity and therefore can be eliminated.

Open-Circuit Voltage: I_o is the parameter in equation (1) which controls the open-circuit voltage. Therefore, its magnitude and variation with material parameters is important. The general form of I_o for any base width is as follows:

$$I_o = qn_i^2\left[\frac{D_n}{N_A L_n} \coth \frac{W_p}{L_n} + \frac{D_p}{N_D L_p} \coth \frac{W_n}{L_p}\right] \tag{2}$$

where n_i is the intrinsic carrier concentration in silicon, $N_A(N_D)$ is the acceptor (donor) concentration, $D_n(D_p)$ and $L_n(L_p)$ are the diffusion constant and the diffusion length of electrons (holes) in the p-(n-) region, $W_p(W_n)$ the width of the base region (diffused region) of the device. The assumptions inherent in equation (2) include an infinite surface recombination velocity at each face and uniform doping density in each region. These latter two assumptions are known to be incorrect for conventional solar cells, and at the present time, it is not possible to estimate the magnitude of error that they introduce.

Materials constants were obtained from the literature (1-7). The cell thickness was fixed at 300 μM and the width of the diffused region at 0.25 μM. Base minority carrier lifetimes were obtained from Iles (2) for resistivities greater than 0.01 Ω-cm, Wolf's data were used for 0.01 Ω-cm. The lifetime in the diffused region was 10^{-8} sec. Table I summarizes the data used and the results of the calculation of I_o. The parameters chosen for the diffused region (i.e. $N_D = 5 \times 10^{19}$, $\mu_p = 20$ cm^2/V-sec, $\tau = 10^{-8}$ sec, W = .25 μM) yield a fixed value for the I_o from the diffused region of 1.2×10^{-14} A/cm^2. This leads to a value of I_o in 0.01 Ω-cm material higher than calculated in references 1 and 2.

Light Generated Current: Wolf (8) has derived a general equation for minority carrier current collected at a n-p junction under illumination. This equation has been programmed for use on a digital computer. A copy of the program was obtained from Wolf and modified slightly to allow additional flexibility. These modifications include calculation of depletion region width using an abrupt junction approximation and the inclusion of spectral reflectance of the surface so that spectral response curves can be calculated as part of the output data.

Values of the light generated current were calculated from this program as a function of both base resistivity and base diffusion length for a standard n^+-p configuration. The surface recombination velocity was chosen to be 10^2 cm/sec at the front of the cell and 10^8 cm/sec at the ohmic rear contact. A complementary error function profile was assumed in the diffused region. In the program, this impurity profile was approximated by two exponential fields. Base doping was uniform and cell thickness was 300 μM. Inclusion of a p^+ drift field at the back contact had only a small effect (~ 2%) on I_o for 10 and 1 Ω-cm resistivities. However, because the equation for I_o does not include the effects of drift fields, they are not presented in this paper. All calculations were performed assuming a totally absorbing silicon surface and the resulting currents were reduced by 5% for a hypothetical uniform antireflecting surface.

Figure 1 shows the variation of short-circuit current with diffusion length calculated with the parameters listed above. There is little increase in current above diffusion lengths of 200 μM as has been noted before in silicon cells. For a constant diffusion length, the current decreases as resistivity decreases because the depletion region gets smaller.

Series Resistance: Series resistance is unavoidable in the conventional solar cell, largely due to the sheet resistance of the diffused layer and the grid finger spacing (9). Measurements of series resistance on cells using standard techniques (10, 11) yielded series resistances about 0.3 Ω. This resistance will lower the power by 3%.

Grid coverage reduces the active area of a solar cell and hence its power output. Present cells have grid coverages between 5 and 10%. The lowest area coverage would come from a wrap-around geometry. Using standard 6-line coverage on a 2 x 2 cm cell the wrap-around geometry would lead to a covered area of 5%. For these calculations then, the cell current was reduced by 5% to account for contact coverage.

Efficiency Calculations: Equation (1) can be solved for short-circuit current, I_{sc}, open-circuit voltage, V_{oc}, and the maximum power point, p_m. The solutions for I_{sc} and V_{oc} are straightforward. The solution for maximum power results in a transcendental equation that can be easily solved by iteration using the Newton-Raphson technique. This solution is especially suited for modern desk-top calculators with memory. Values of I_o calculated from equation (2) and values of I_L obtained from figure 1 were used. The values of I_L on figure 1 were reduced by 5% to account for the coverage of the grid as noted above. The resulting values of p_m and efficiency were then reduced by 3% to account for a 0.3 Ω series resistance. The values of V_{oc}, I_{sc} and efficiency so calculated are shown in figure 2. The peak efficiency is about 18% occurring for a base resistivity between 0.1 and 0.01 Ω-cm. Table II lists the performance obtained for the various resistivities. The maximum efficiency is slightly lower than that reported by Wolf (1) because of higher loss values chosen for reflectivity (5% to his 3%) and grid area coverage (5% to 0%) and the higher I_o value calculated for 0.1 Ω-cm material.

In summary, for a simple planar p-n junction model, a practical upper limit of silicon solar cell efficiency of 18% has been obtained for 0.1 Ω-cm material.

Radiation Damage

Diffusion Length Degradation: Estimates of the performance of these high efficiency cells in a radiation field were made using the standard model for diffusion length degradation:

$$\frac{1}{L^2} = \frac{1}{L_o^2} + K\Phi$$

where L is the diffusion length after some fluence Φ, L_o is the initial diffusion length and K is a damage coefficient for the bombarding particle and the semiconductor material. For this calculation synchronous orbit was assumed as was the damage integral (KΦ) as calculated by Cooley and Barrett (12) for 10 Ω-cm material covered with .015 cm fused silica ($K\Phi = 4.12 \times 10^3$/cm^2- year). It was assumed that the cover glass used did not lower the initial short-circuit current. The damage integral so calculated assumes the damage to be caused by solar flare protons and trapped electrons.

The problem of determining damage integrals at other resistivity values is a bit more difficult. From data of Denney and Downing (12, 13, 14), it was estimated that the damage integral for 1 Ω-cm silicon material was about 3-5 times that of 10 Ω-cm material. For this calculation, the worst case was chosen (i.e., $K\Phi = 2.06 \times 10^4/\text{cm}^2\text{-yr}$). Below 1 Ω-cm material, however, almost no data are available. Curtis and Srour (15) present data on neutron-irradiated material which indicate that the damage coefficient becomes constant from 1 Ω-cm to lower resistivities. Because there is a general correspondence between neutron and proton or electron damage in silicon, the damage integral was assumed to remain constant at $2.06 \times 10^3/\text{cm}^2\text{-yr}$ for resistivities 1 Ω-cm and below.

Performance Calculation: The change in diffusion length determined from equation (3) was used to calculate both an I_o from equation (2) and a light generated current from figure 1. These data were then used to determine cell parameters using equation (1) and the corrections previously noted. Figure 3 shows the results of these calculations. Also included are the calculated values for a present-day 10 Ω-cm cell and some data obtained after 1.1 and 3.3 years (16, 17) in synchronous orbit for conventional cells. These latter data demonstrate the general validity of the calculations. It can be seen that all of the "advanced" cells are significantly higher in efficiency than the present day cell at all times. The advantage comes largely from better collection efficiency, optical coatings and fill factor. Due to its higher damage coefficient, the efficiency of the 1 Ω-cm cell falls below that of the 10 Ω-cm cell after about 5 years in orbit.

PATHS TO IMPROVE EFFICIENCY

Characteristics of present solar cells were examined in the light of the same theory and assumptions used to calculate the ultimate efficiency. The purpose was to assess what areas of improvement offer the most gain in efficiency and what knowledge must be acquired to realize improvements in these areas.

Improvements in Short-Circuit Current

As can be seen from figure 1, increasing the diffusion length from 150 to 600 μM in the silicon solar cell produces only about a 1 mA/cm^2 increase in cell output. Therefore, greatly increased diffusion lengths will not greatly increase cell output. Furthermore, the diffusion lengths in 0.1 Ω-cm material are on the order of 90 μM ($\tau = 4$ μsec) (18), leading to currents within 10% of the maximum achievable. Hence, major efforts to increase the diffusion length in this material would not produce large increases in output.

The measured spectral response of a 10 Ω-cm, uncoated, 0.25 μM junction silicon solar cell is shown in figure 4. An insight into some of the materials parameters can be obtained by fitting this response with the theory described previously. The response of the cell in the infrared spectral region is strongly dependent on diffusion length. A value of 170 μM was obtained on the data shown. Direct measurement of the diffusion length by the X-ray technique (19) yielded a value within 5% of that obtained by fitting. As can be seen, however, it was not possible to fit the blue response of the cell by assuming a complementary error function for the impurity profile in the diffused region. Only by using the anomalous profile noted by Iles and Liebenhaut (20) could satisfactory agreement be obtained. A front surface recombination velocity of 10^5 cm/sec was used. Subsequent measurements at NASA-Lewis of the impurity profiles in similarly processed cells have indicated the presence of an anomalous profile.

The response of a cell to blue wavelengths of light is significantly reduced when both an anomalous profile and a high surface recombination velocity are present. An example of this effect is shown in figure 5, where the calculated response at 0.4 μM of a SiO-coated silicon cell is shown for various values of S and diffused impurity profile. It appears that a significant increase in output of a solar cell could be achieved by obtaining a complementary error function profile even if S were to remain high. Calculations show that this increase would amount to nearly 3 mA/cm^2. Conceivably, if an error function profile were achieved, S might also be reduced because of the resulting improvement in perfection of the surface; however, subsequent reduction of S to 10^2 cm/sec would add less than 0.5 mA/cm^2 to the cell output.

Improvements in Open-Circuit Voltage

The key to obtaining significant increases in solar cell efficiency lies in obtaining large increases in the open-circuit voltage by reducing the resistivity. The open-circuit voltage is strongly related to I_o (for a given I_L). Simple diffusion theory was used to predict the behavior of cell open-circuit voltage for a conventional 10 Ω-cm cell with temperature. The results of this calculation are shown in figure 6. Performance data were taken from previously published work (21). Since excellent agreement is obtained, it appears that the open-circuit voltage of 10 Ω-cm cells can be adequately described by simple diffusion theory with unity A values.

It has, however, been noted by Iles (2), that the open-circuit voltage of cells does not continue to increase as the resistivity decreases as expected from diffusion theory. Instead, the open-circuit voltage saturates at about 0.62 V for resistivities lower than 1 Ω-cm. This voltage difference cannot be attributed to poor bulk minority carrier lifetimes. Iles (18) has found that 0.1 Ω-cm cells with diffusion lengths of 90 μM can show open-circuit voltages in the 0.55-0.6 V range. To better understand the reason for this loss in voltage, the forward diode characteristics were obtained on both 10 and 0.1 Ω-cm cells. Iles also etched small mesa regions (10 to 20 mesas each with a diameter of 0.145 cm per wafer) into several of these 0.1 and 10 Ω-cm cells to sample the distribution of characteristics over the surface. The results of these measurements are shown in figure 7 where envelopes encompassing the typical range in performance for both resistivity materials are shown. A line at a current density of 35 mA/cm^2 (equivalent to sunlight illumination) is provided for reference. The large excess forward currents noted at low forward voltages are high enough to significantly reduce the open-circuit voltage in 0.1 Ω-cm material below that expected. The variation from spot to spot is also quite large. In 10 Ω-cm material both the magnitude and variability of the excess forward current is less than for the 0.1 Ω-cm case. Accordingly, there is no loss in open-circuit voltage over that predicted. (There is a small loss in maximum power, however.)

The mechanism giving rise to this excess forward current is not clear at the present time. Possible explanations for this effect include current loss through defect regions in the diffused layer and junction and surface or edge leakage currents around the junction. The increase in efficiency predicted earlier depends strongly on increased open-circuit voltage in low resistivity material. Therefore, it is imperative that the cause of this excess forward current be understood and eliminated so these gains can be achieved.

Improvements in Theory

Increased open-circuit voltages (.58-.585 V) have been reported for n^+-p-p^+ solar cell structures made from 10 Ω-cm material (2, 22, 23). These voltages are significantly in excess of the 0.55 V maximum open-circuit voltages seen in conventional cells. The use of simple diffusion theory to obtain I_o as outlined previously does not explain these high voltages, even when long minority carrier lifetimes are used. Equation (2) was derived on the basis of uniform doping in both regions. Therefore it is not entirely surprising that it does not predict the voltage in the n^+-p-p^+ case, where significant doping variations are present. Before these higher open-circuit voltages can be explained, the diffusion expression for I_o must be rederived for the more general case with arbitrary doping profiles. The further insight gained from this work may lead to further increases in cell output.

COMMENTS AND CONCLUSIONS

Calculations indicate that a potential increase in efficiency of silicon solar cells to near 18% may be achievable through the use of low resistivity material possessing good diffusion lengths, diode characteristics and improved surfaces and diffusion profiles. Further, the calculations indicate that these cells should be superior to present day silicon cells in a synchronous radiation environment.

Analysis of conventional cells, however, discloses a number of problem areas that must be studied further in order to achieve higher outputs. The increases in short-circuit current that may be achievable in the cell are rather modest. Because the diffusion lengths in present cells (both 10 and 0.1 Ω-cm) are long, only minor increases in current could be expected from large increases in diffusion length. Increases in the blue response of cells can be achieved by elimination of an anomalous impurity diffusion profile in the diffused region. If a complementary error function profile were obtained, calculations show that an increase of nearly 3 mA/cm^2 could be achieved even if the surface recombination velocity were to remain high.

The measured open-circuit voltages of low resistivity material are much lower than predicted by diffusion theory. This loss is not due to poor diffusion lengths. Rather it is due to excess forward diode currents. In order to achieve the large anticipated increase in open-circuit voltage for low resistivity material, the origin of this excess current must be determined and eliminated.

Although simple diffusion theory yields open-circuit voltage in agreement with practice for conventional 10 Ω-cm n^+-p cells it does not yield satisfactory results for more complex structures such as the n^+-p-p^+ cell. Increased theoretical understanding of these cells may lead to further insights that may yield additional improvements in the output of solar cells.

Thus a variety of problem areas that limit increased output from silicon solar cells has been outlined. An agressive program aimed at these problems can be expected to either yield increased output or at least an understanding of the ultimate limits of efficiency in the silicon solar cell.

REFERENCES

1. Wolf, M.: Conference Record of the 8th IEEE Photovoltaic Specialists Conference, Seattle, Washington, August 1970, p. 360.

2. Iles, P.: Conference Record of the 8th IEEE Photovoltaic Specialists Conference, Seattle, Washington, August 1970, p. 345.

3. Barber, H. D.: Solid State Electronics 10, pp. 1039-1051, 1967.

4. Prince, M. B.: Phys. Rev. 93, pp. 1204-1206, 1954.

5. Backenstoss, G.: Phys. Rev. 108, pp. 1416-1419, 1957.

6. Gärtner, W. W.; Proc. IRE 45, pp. 662-680, 1957.

7. Irvin, J. C.: Bell System Tech. J. 41, p. 387, 1962.

8. Wolf, M.: Proc. IEEE 51, pp. 674-693, 1968.

9. Handy, R. J.: Sol. St. Elect. 10, 765-775, 1967.

10. Wolf, M.; and Rauschenbach, H.: Adv. Energy Conv. 3, pp. 455-579, 1963.

11. Imamura, M. S.; Portscheller, J. I.: Conference Record of the 8th IEEE Photovoltaic Specialists Conference, Seattle, Washington. August 1970, p. 102.

12. Cooley, W. C.; and Barrett, M. J.: Handbook of Space Radiation Effects on Solar Cell Power Systems, Contract NASw-1345, January 1968.

13. Denny, J. M.; and Downing, R. G.: Charged Particle Radiation Damage in Semiconductors: IX Proton Radiation Damage in Si, Final Report, Contract NAS5-1851, August 1963.

14. Denny, J. M.; and Downing, R. G.: Charged Particle Radiation Damage in Semiconductors: X Energy Dependence of Electron Damage in Si, Contract NAS5-3805, September 1964.

15. Curtis, O. L., Jr.; and Srour, J. R.: Proceedings of the Fourth Annual Conf. on Effects of Lithium Doping on Silicon Solar Cells, Jet Propulsion Laboratory Technical Memorandum 33-491, pp. 65-70, September 15, 1971.

16. Waddel, R.: Proceedings of the 7th IEEE Photovoltaic Specialists Conference, Pasadena, California, Nov. 1968, p. 195.

17. Grant, R. J.: Flight Data Analysis of Power Subsystem Degradation at Near Synchronous Altitude, Second Quarterly Report, Contract NASw-1846, Philco Ford Corp. #TR-DA2159, January 1970.

18. Iles, P.: Private Communication, NASA Contract NAS3-15689, Effects of Processing on minority Carrier Lifetime in Silicon Solar Cells.

19. Lamneck, J. H.: Diffusion Lengths in Silicon Obtained by an X-ray Method, NASA TM X-1894, October 1969.

20. Iles, P.; and Liebenhaut, B.: Solid State Elect. 5, pp. 331-339, 1962.

21. Brandhorst, H. W., Jr.; and Hart, R. E., Jr.: Effects of Decreasing Temperature and Illumination Intensity on Si Solar Cell Performances, NASA TM X-52756, Feb. 1970.

22. Mandelkorn, J.; and Lamneck, J. H.: A New Method for Fabrication of Thin Silicon Solar Cells and Their Characteristics, Proceedings of the 9th IEEE Photovoltaic Specialists Conference, Silver Spring Maryland, 1972.

23. Fischer, H.; Link, E.; and Pschunder, W.: Proceedings of the 8th IEEE Photovoltaic Spec. Conf., Seattle, Washington, p. 70, August 1970.

CALCULATED SHORT CIRCUIT CURRENT DENSITY AS FUNCTION OF RESISTIVITY

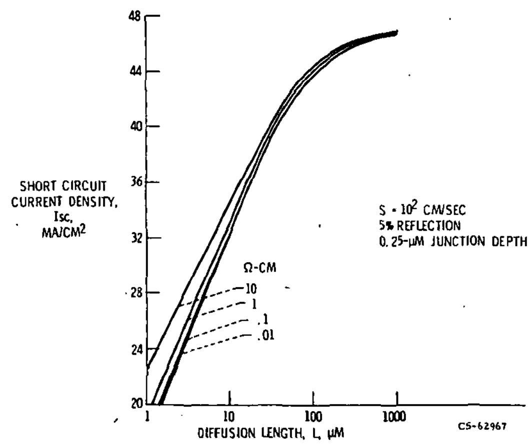

Fig. 1.

CALCULATED PERFORMANCE OF SILICON SOLAR CELLS AS FUNCTION OF RESISTIVITY

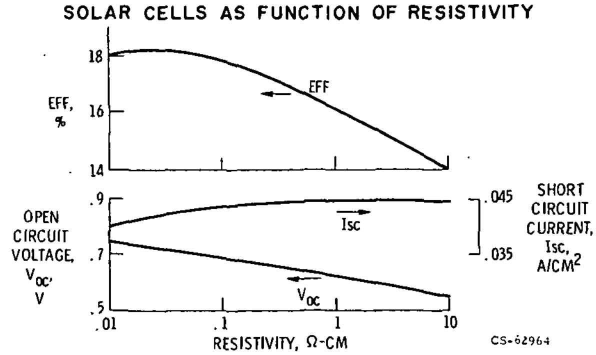

Fig. 2.

CALCULATED DAMAGE TO ADVANCED SOLAR CELLS IN SYNCHRONOUS ORBIT

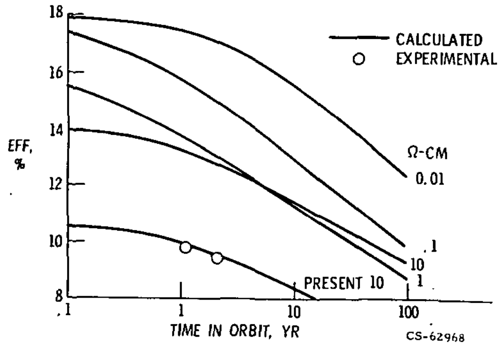

Fig. 3.

VARIATION OF OPEN-CIRCUIT VOLTAGE OF 10Ω-CM N/P SILICON SOLAR CELL

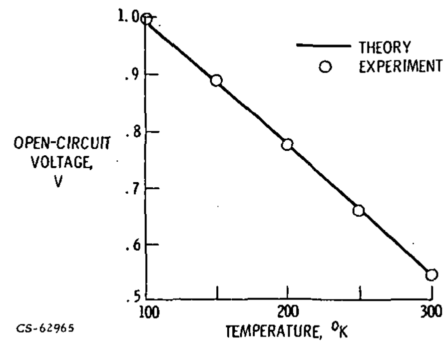

Fig. 6.

SPECTRAL RESPONSE OF 10Ω-CM SILICON SOLAR CELL

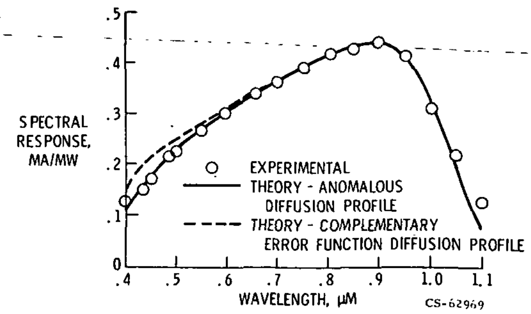

Fig. 4.

FORWARD DIODE CHARACTERISTICS OF MESAS MADE ON 10 AND 0.1Ω-CM SOLAR CELL MATERIAL

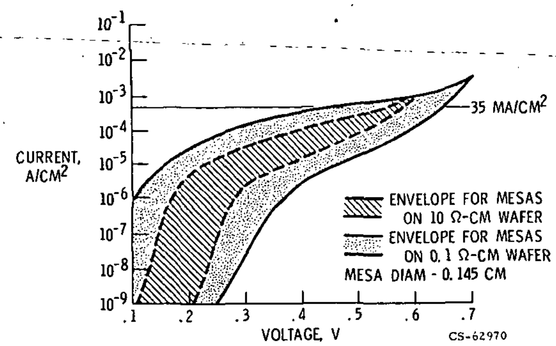

Fig. 7.

CALCULATED SPECTRAL RESPONSE AT 0.4μM OF SiO COATED SILICON SOLAR CELL

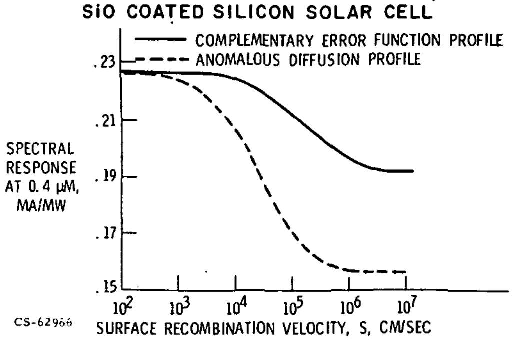

Fig. 5.

TABLE I

CALCULATION OF SATURATION CURRENT DENSITY FOR n^+-p SILICON SOLAR CELLS

RESISTIVITY	MAJORITY CARRIER CONCENTRATION N_A, cm^{-3}	MINORITY CARRIER MOBILITY μ, cm^2/V-sec	MINORITY CARRIER LIFETIME (BASE) τ, sec	SATURATION CURRENT DENSITY I_o, A/cm^2
10	1.35×10^{15}	1300	1×10^{-4}	2.64×10^{-11}
1	1.6×10^{16}	1100	8×10^{-5}	2.00×10^{-12}
0.1	4.6×10^{17}	800	3×10^{-5}	1.47×10^{-13}
.01	1.1×10^{19}	160	1×10^{-5}	1.37×10^{-14}

TABLE II

CALCULATED PERFORMANCE OF ADVANCED SILICON SOLAR CELLS

	Present Cells	ADVANCED CELLS			
Bulk Resistivity, ρ, Ω-cm	10	10	1	0.1	.01
Short-Circuit Current, I_{sc}, A/cm^2	.037	.0442	.0441	.0433	.0399
Open Circuit Voltage, V_{oc}, V	.545	.550	.616	.683	.742
Fill Factor, F.F.	.72	.792	.806	.817	.827
Efficiency, %	10.7	14.1	16.1	17.8	18.0